Structured Generation Method of 3D Synthetic Tree Models for Precision Assessment

Zhuoyu Ao[1], Weixi Wang[1], Yaoyu Li[1], Hongsheng Huang[1],Xiaoming Li[1], Renzhong Guo[1],Shengjun Tang[1]

[1] Research Institute for Smart Cities, School of Architecture and Urban Planning, Shenzhen University, Shenzhen, P.R. China

Keywords: Synthetic datasets, 3D Tree Modeling, Point cloud, Skeleton Extraction.

Abstract

The technology for 3D reconstruction of tree models based on point clouds has been extensively researched, necessitating effective datasets for the study of branch and leaf separation, skeleton point extraction, and tree parameter extraction methods. However, existing datasets for 3D tree models face several challenges, including insufficient data volume for deep learning network training, low accuracy of model ground truth impeding effective method precision evaluation, and a lack of dataset richness to satisfy the needs of multi-type method assessments. In response to these challenges, This paper introduces, for the first time, a fully automated method for generating structured three-dimensional synthetic tree models, and constructs a large-scale 3D synthetic tree dataset enriched with comprehensive structural information. This method facilitates automated computation across several processes, including the mass generation of simulated trees, separation of branches and leaves, noise generation, extraction of skeleton points, and volume calculation. To validate the usability of this dataset across various applications, this paper employs state-of-the-art (SoTA) algorithms to verify the accuracy of methods in 3D tree model reconstruction and carbon stock calculation, thereby thoroughly demonstrating the dataset's effectiveness.

1. Introduction

The technology for 3D reconstruction of tree models based on point clouds has been extensively studied, involving complex processes such as branch and leaf separation (Ferrara et al., 2018), skeleton point extraction (Vega et al., 2014, Liu et al., 2021), and tree parameter extraction(Putman and Popescu, 2018). Effectively evaluating the accuracy and effectiveness of various methods in the tree 3D reconstruction process is crucial for continually enhancing algorithm precision and usability. Three-dimensional tree datasets, fundamental to tree-related applications, offer vital reference information for the training processes and accuracy assessment of various algorithms. Different algorithms, however, have varying requirements for the volume and richness of dataset information. For instance, the precision of deep learning-based tree part segmentation algorithms significantly depends on the dataset size(Liu et al., 2021), while tree volume calculations require datasets containing volume ground truth(Kankare et al., 2013). Similarly, accurate tree point cloud ground truth is essential for assessing the geometric precision of trees in 3D. It can be said that large-scale tree datasets are instrumental in enhancing the accuracy and reliability of algorithms related to 3D tree computation and analysis.

There are many current studies on point cloud reconstruction. AdTree (Du et al., 2019) uses Dijkstra's shortest path algorithm to build a minimum spanning tree to obtain an initial tree skeleton, then prunes the initial tree skeleton and performs an optimization-based method to fit a series of cylinders to approximate the geometry of the tree branches. The algorithm is validated using publicly available point cloud datasets, which come from different sources, have different formats, contain noise, and suffer from missing data. Hu et al. (Hu et al., 2017) proposed an efficient tree modeling to enrich sparse point clouds by adding new backbone points and simulating direction fields, thus realizing reconstruction of natural tree skeleton from sparse data. The data set of this method were acquired by an airborne LiDAR scanning system, which required manual acquisition and processing of single tree segmentation. Mei et al. (Mei et al., 2017) present a L1-minimum spanning tree (MST) algorithm to refine tree skeletons from the optimized point cloud, which integrates the advantages of both L1-median skeleton and MST algorithms. In this study, a single tree collected by ground-based laser scanning was used for qualitative and quantitative evaluation, and the tree samples collected were small, with few species and not comprehensive.

Addressing the aforementioned challenges, this paper presents the structured generation method of 3D synthetic tree models for precision assessment. The paper first outlines an automated method for hierarchical construction of simulated tree models, allowing for the mass reconstruction of large-scale synthetic trees. Subsequently, for individual tree models, a technical system is developed to provide comprehensive outputs including tree point clouds, skeletons, and volume data. As the first large-scale, multi-type synthetic tree model dataset, this paper validates the accuracy of methods for 3D tree model reconstruction and carbon stock calculation using state-of-the-art (SoTA) algorithms, thereby thoroughly demonstrating the dataset's effectiveness.

2. Methodology

2.1 Overview of the framework

This paper introduces a novel fully automated method for generating structured three-dimensional synthetic tree models and constructs a large-scale 3D synthetic tree dataset with comprehensive structural information. As shown in Figure 1, in the realm of 3D synthetic tree model construction, an integrated and automated technological process has been established. This process encompasses the mass generation of 3D synthetic trees, separation of branches and leaves, noise generation, and extraction of skeleton points (including diameter calculation and hierarchical relationship restoration), leading up to volume calculation. Initially, a parametric structural description is employed,

along with an adaptive parameter adjustment method, to build a library of batch 3D synthetic tree models. Building on this, the paper delves into the separation of branches and leaves, the division of tree hierarchical structures, and explores methods for the automatic generation of tree point clouds, automatic extraction of skeleton structures and parameter information, as well as the computation of volume ground truth. Utilizing this methodology, a dataset comprising tens of thousands of 3D synthetic tree models has been constructed for the first time.

2.2 Synthetic tree generation

Generation of single synthetic tree: As shown in Figure 2, to acquire three-dimensional tree models with hierarchical structures, this paper adopts a manual modeling approach for parametric modeling of individual trees. Following the distinct growth logic of different tree species, a hierarchical organization method is employed, ranging from the tree's main trunk through multiple levels of branching to the leaves, facilitating adaptive growth and the acquisition of complete 3D tree models. Since the tree models constructed in this study are generated based on parametrization, various tree parameters, including phototropism, leaf quantity and distribution, droop, height, and thickness, can be adjusted. This adaptability lays a critical foundation for subsequent automated batch generation. Each tree model encompasses five levels of branches and foliage information, along with detailed bark and leaf texture mapping.

Batch generation of synthetic trees using parameterized adjustments: Based on manually modeled trees, this paper proposes a batch generation method for tree models using parameterized adjustments. As illustrated in Figure 3 starting with an individual tree, random adjustments are made to parameters such as phototropism, noise, gravity, height, angle, and sparsity. This process allows for the batch generation of 3D models of the same tree species, each exhibiting varying morphologies and structures. For a single tree species, the method automatically generates 1,300 trees, with each tree containing approximately 100-3,000 branches and 700-40,000 leaves, depending on the species. The batch-generated synthetic tree models, created using this method, will be utilized in the subsequent construction of datasets.

2.3 Generation of semantically rich tree point clouds

Branch and leaf separation and point cloud generation: Utilizing the parametric simulation method for tree reconstruction, this paper achieves the acquisition of complete three-dimensional tree models. These models possess detailed hierarchical structural information, including the tree trunk, leaves, branch sequence, and texture details. Leveraging the rich semantic and hierarchical information within these models, this study conducts individualized segmentation of all branches and performs branch and leaf separation. The result is the generation of three-dimensional point cloud data with separated branches and leaves, as well as individualized branches.

To achieve these objectives, the paper first traverses the leaf and branch components within the triangular mesh model. By interpreting the semantics of the triangular mesh, all branches and leaves are merged to create a separated triangular mesh model of branches and leaves. Subsequently, for accurate tree point cloud data acquisition, the paper utilizes the triangular mesh as a base to voxel-fill (with a filling density of 0.01m) the 3D models of branches and leaves, thereby obtaining corresponding dense 3D point cloud data. The point clouds obtained for different tree species vary, with the number of branch and leaf point clouds ranging approximately between 800,000 and 10,000,000. Considering the errors inherent in actual measurement processes, Gaussian noise was added to the generated branch and leaf point clouds, and noisy point cloud data was concurrently produced to enhance the realism of the point clouds.

Attribution of semantic information to tree branches: To meet the requirements of precise tree reconstruction accuracy assessment and clustering accuracy evaluation, this paper effectively extracts and outputs information about each point's corresponding branch and the hierarchical relationship of the branch point clouds, in addition to the complete point clouds of branches and leaves. Specifically, while traversing the 3D model of each branch, the study records the index information of each branch and its hierarchical level. During the voxel sampling of the point cloud, the corresponding attributes are assigned to the cloud. As shown in Figure 4, different colors in (c) represent different branch information, which can be used to evaluate the effectiveness of branch clustering methods. In (d), different colors indicate the hierarchical levels of branches, determined by the branching of the tree, with the lowest level being 1 and the highest level being 5 in this study.

2.4 Skeleton Generation and Annotation

To meet the requirements for precise extraction of three-dimensional tree reconstruction skeleton points and accurate assessment of carbon storage calculation methods, this paper proposes an automated and accurate method for generating skeleton points of synthetic tree models. This method, based on the original tree models, automatically extracts the central axis of the branches to obtain accurate skeleton points, and slices the branches to acquire precise radius information. Subsequently, branch indices, hierarchical relationships, and radius information are output as attributes of the skeleton points.

Skeleton point extraction: For the branch structures in the tree models, each branch's point cloud is computed through principal component analysis. The normal information of the slicing plane is determined based on its maximum eigenvector, which represents the growth direction of the tree. This plane orientation ensures that the skeleton points conform to the tree's growth trend. As depicted in Figure 5(a), (b), (c), and (d), starting from the bottom of the branch, the branch is sliced at intervals of 0.01 meters, and the resulting point clouds are projected onto the slicing plane. The center coordinates of the projected point cloud are calculated and used as the skeleton point for that segment. This slicing process continues from the bottom to the top of the branch until all skeleton points are calculated. The same method is applied to obtain skeleton information for other branches.

Attribute information generation: Section 2.2 provides each branch's index and hierarchical information, which can directly serve as attributes for the branch's skeleton points. However, precise carbon storage calculation requires accurate volume information, making the tree's radius crucial. Therefore, as shown in Figure 5 (e), based on the point cloud data obtained from slice projections, the distance between each projected point and the center point is calculated, and the average distance is taken as the radius of the current tree skeleton point. This radius information will serve as the radius attribute of the tree skeleton.

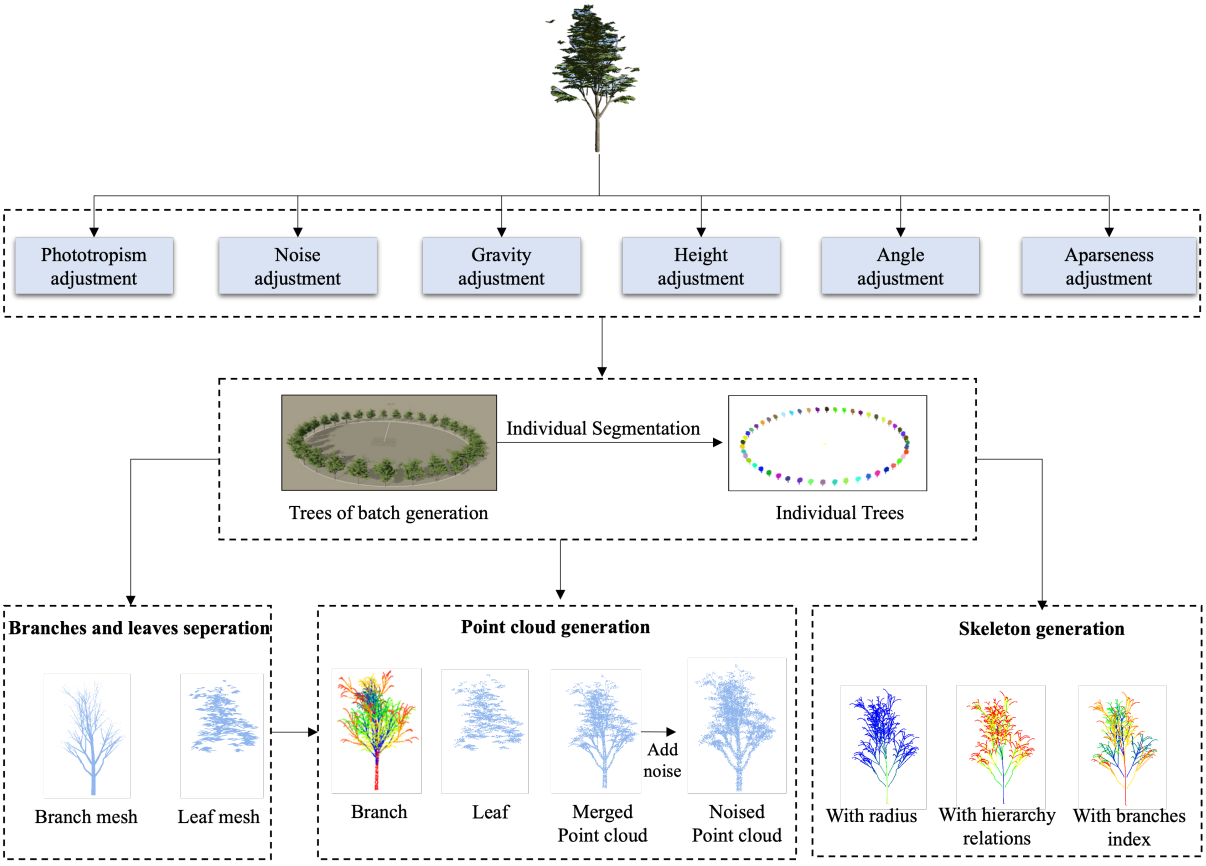

Figure 1. Overview of the proposed tree reconstruction method.

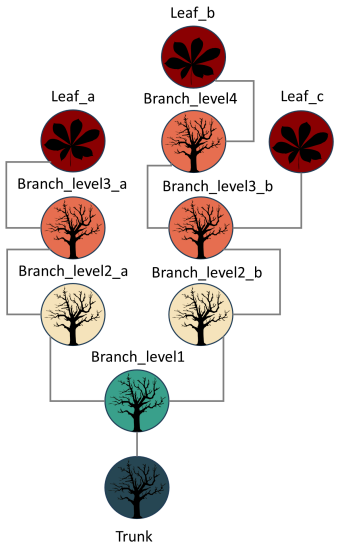

Figure 2. Branch and leaf structure of small-leaved olive.

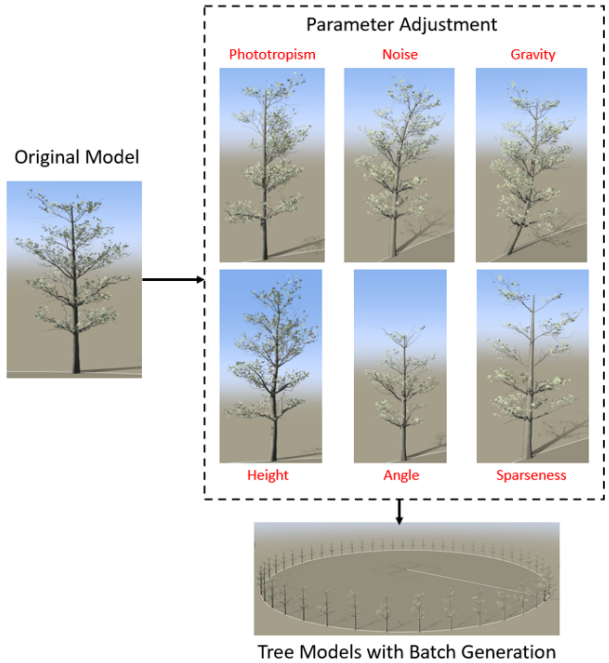

Figure 3. The process of batch tree generation.

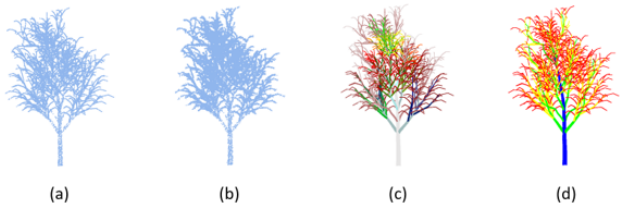

Figure 4. Adding noise to the point cloud and recording attributes to the point cloud. (a)Original point cloud. (b)Noise point cloud. (c)Point Cloud-Branch Index. (d)Point Cloud-Branch Hereditary Relations.

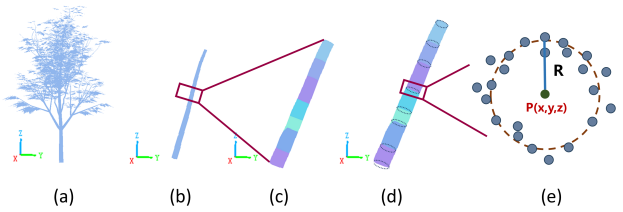

Figure 5. Calculation process for skeleton points and radius. (a)Tree mesh model . (b)Traverse the branches. (c)Cut in the optimal direction. (d)Local cross section . (e)Acquired center of mass and radius.

Figure 6 displays the results of skeleton point generation, showing the original tree model, skeleton points with radius attributes, skeleton points with trunk hierarchical relationship, and skeleton points with branch index. Attribute values are differentiated by various colors.

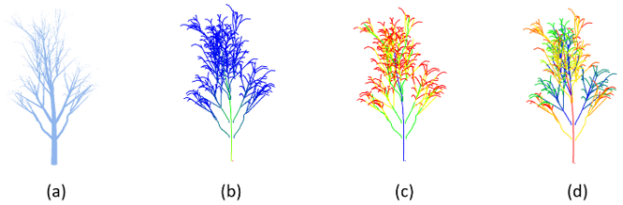

Figure 6. Calculation of skeleton points based on branch mesh model. (a)Mesh model. (b)Skeleton-Radius. (c)Skeleton-Branch Hereditary Relations. (d)Skeleton-Branch Index.

3. Experiments and Analysis

In order to assess the effectiveness of the large-scale synthetic 3D tree model dataset constructed in this study for various applications and algorithm performance evaluations, the paper will utilize two types of applications including tree 3D reconstruction and tree volume calculation to evaluate the usability of the information in the dataset. Additionally, using this dataset as a foundation, the study will accurately assess the precision of different algorithms within the same application scenarios.

3.1 Synthenic Tree Reconstruction

This comprehensive dataset features simulation models of ten common tree types, including fir (Cunninghamia lanceolata (Lamb.) Hook.), camphor (Camphora officinarum Nees ex Wall), small-leaved olive (Ficus obliqua), ajang olive (Terminalia arjuna), flamboyant tree (Delonix regia), agarwood (Aquilaria malaccensis), flooded gum (Eucalyptus grandis), lemon tree (Citrus × limon (Linnaeus) Osbeck), Lombardy poplar (Lombardy poplar), and Tibetan cherry (Prunus serrula Franch. var. tibetica (Batal.) Koehne). Each unique in morphology and structure, with leaves, branches, and bends created through parametric manipulation. Figure 7 illustrates examples of three species: flamboyant tree, camphor tree, and ajang olive. The dataset provides a comprehensive suite of data for each tree species, including complete point clouds, noise-added point clouds, leaf meshes, branch meshes, leaf point clouds, branch point clouds (each with attributes to distinguish individual branches), and skeleton points with attributes such as radius, branch hereditary relations, branch index, and total branch volume. Additionally, two types of point clouds, with and without noise, are included to facilitate the evaluation of computational accuracy in processes like tree skeleton point computation, tree reconstruction, tree carbon storage calculation, and tree part segmentation.

3.2 Accuracy evaluation of tree reconstruction methods

Data description: This study selected five tree species for testing: fir, camphor, small-leafed olive, ajang olive, and flamboyant trees. Two trees from each species were chosen, incorporating both real and noisy point clouds. This resulted in a total of 20 tree branch point clouds for tree reconstruction tests. All data were downsampled to 100,000 points per tree, with an average of approximately 900 branches per tree. The test trees varied in height, ranging from 10m to 150m.

Method: The validity of the dataset was assessed using three prevalent algorithms: AdQSM (Fan et al., 2020), AdTree (Du et al., 2019) and TreeQSM (Raumonen et al., 2013), for computing Tree Models, Tree Skeletons, and Tree Carbon Storage. AdTree employs the Dijkstra shortest path algorithm for initial tree skeleton extraction from point clouds, followed by pruning redundant components and fitting cylindrical models to approximate tree branch geometry. AdQSM refines this process by using the average radius of three non-overlapping trunk sections to establish the initial cylindrical radius. TreeQSM, on the other hand, reconstructs the visible tree surface with a flexible cylindrical model, recording the tree’s topological branching structure in its quantitative model.

Metrics: The study utilized the Hausdorff distance algorithm for a quantitative comparison of the reconstructed mesh models against ground-truth skeleton points and tree mesh models. The Hausdorff distance, a measure of the extent to which two subsets of a metric space diverge, is defined as:

$$H(A,B) = max\left\{(A,B), h(B,A)\right\} \tag{1}$$

Among them,

$$h(A,B) = \max_{a\in A}\left\{\min_{b\in B} \parallel a-b \parallel\right\} \tag{2}$$

$$h(B,A) = \max_{b\in B}\left\{\min_{a\in A} \parallel b-a \parallel\right\} \tag{3}$$

The algorithm’s performance was evaluated in terms of both relative and absolute errors.

3.2.1 Results of Tree model

In this study, we conducted a comprehensive evaluation of three-dimensional tree reconstruction accuracy using point clouds from five synthetic tree species, applying three distinct

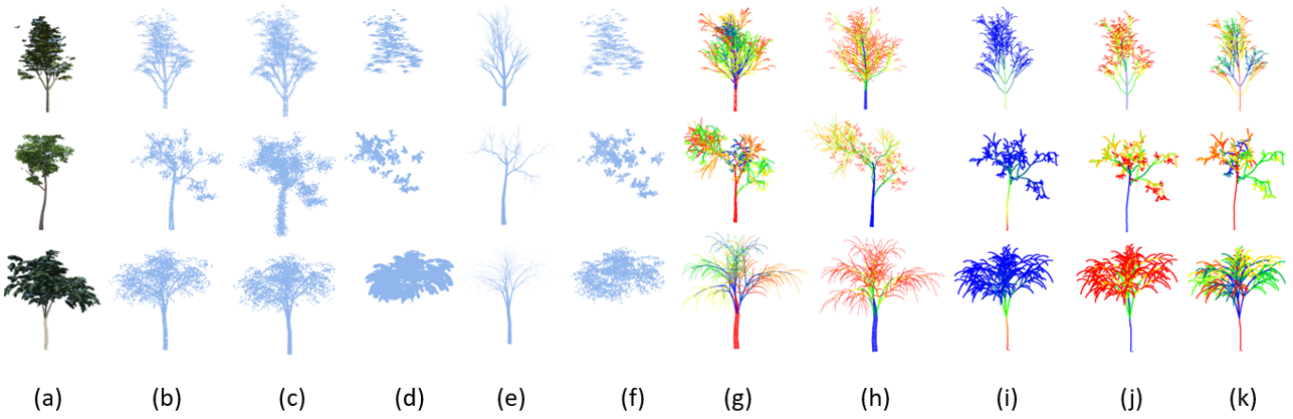

Figure 7. TreeNet3D dataset. (a)Original Mesh. (b)Complete Point Cloud. (c)Noise Point Cloud. (d)Leaf Mesh. (e)Branch Mesh. (f)Leaf Point Cloud. (g)Branch Point Cloud-Part Segmentation. (h)Branch Point Cloud-Hereditary Relations. (i)Skeleton-Radius. (j)Skeleton-Hereditary Relations. (k)Skeleton-Branch Index.

reconstruction methods: AdQSM, AdTree, and TreeQSM. The precision of each reconstruction method was meticulously assessed to demonstrate the capability of our dataset in evaluating 3D tree reconstruction algorithms.

The accuracy of tree reconstructions was primarily evaluated against the ground-truth Mesh model of each tree.To facilitate this, all meshes were sampled into point clouds containing 100,000 points. The nearest neighbor distances between the actual ground results and the reconstructed results were compared to measure accuracy. Table 1 presents a detailed analysis of the absolute and relative errors in tree model reconstruction accuracy for various tree species, both in the absence of noise and under its influence. It was observed that the Phoenix tree, having the highest average height, exhibited the poorest overall modeling accuracy, while the Small-Leafed Olive tree, with the lowest average height, showed better results. This discrepancy is attributed to the height variation among tree species. Hence, the modeled error distances are normalized by dividing by the height of the tree itself. The TreeQSM method displayed higher calculation accuracy overall. However, discrepancies in reconstruction accuracy were noted among different tree species, potentially due to variations in tree morphology or specific optimization decisions within the reconstruction algorithms. Generally, trees with more branches and trunks tended to have poorer modeling accuracy, whereas those with fewer mid-trunks showed relatively better accuracy. The impact of noise on tree reconstruction varied across different tree species and reconstruction methods. For instance, noise had a relatively minor effect on the reconstruction of camphor trees across all methods, whereas it significantly increased the average error for all reconstruction algorithms when reconstructing Ajeng olive trees. The sensitivity of reconstruction methods to noise is dependent not only on the algorithm itself but also on the specific tree type.This analysis substantiates the proposed dataset’s capability to effectively assess tree reconstruction algorithms, highlighting the varying influences of tree complexity, height, and noise on algorithm performance.

3.2.2 Results of Tree Skeleton

We conducted an in-depth evaluation of the accuracy of skeleton point modeling in three-dimensional tree reconstruction using point clouds from five synthetic tree species. This evaluation utilized three different reconstruction methods: AdQSM, AdTree, and TreeQSM. Our goal was to assess the precision of skeleton points in the reconstructed trees and to demonstrate the capability of our dataset for evaluating the accuracy of tree skeleton point algorithms. To verify the accuracy differences among AdQSM, AdTree, and TreeQSM for skeleton point modeling, we performed a comparative analysis between the real skeleton points provided in the dataset and the results computed during the tree reconstruction process.

Table 1 details the mean absolute error for each tree skeleton point, both with and without added noise. To account for the influence of tree height on nearest proximity distance error, the modeling error distance was normalized by dividing by the respective tree height, enabling the calculation of relative error for skeleton point computation. From the results, it is evident that different methods yielded similar accuracy to the tree Mesh model. However, the modeling error for the fir tree was larger, while the Phoenix canariensis exhibited the best overall modeling accuracy. This variance is consistent with the previous conclusion that the simplicity of branches affects modeling accuracy. TreeQSM demonstrated higher precision in calculating skeleton points, whereas AdTree showed the least precision. When examining the impact of noise on algorithm accuracy, camphor trees were less affected by noise, whereas fir trees were the most affected. This outcome aligns with the mesh model results, primarily due to differences in the basic shape of trees. Overall, AdQSM displayed better resistance to noise compared to the other two algorithms.

4. Conclusions

This study presents the structured generation method of 3D synthetic tree models for precision assessment. Based on the parametrically generated tree models, different parameters were randomly adjusted to batch generate 3D models of different tree species. Based on the detailed semantic and hierarchical information, pioneering large-scale synthetic tree dataset was generated. The dataset stands as the first artificial tree dataset of this scale and detail, providing a substantial contribution to the field. The dataset’s versatility extends to a wide array of deep learning tasks, offering a realistic training set for objectives such as tree segmentation, species classification, branch and leaf separation, part segmentation, skeleton point extraction, tree reconstruction, and carbon stock prediction. Beyond tree reconstruction, the dataset supports a variety of downstream applications, significantly enhancing the realm of 3D

Table 1. Tree model accuracy and Tree Skeleton Accuracy

Error	Tree Index	Tree model accuracy			Tree Skeleton Accuracy		
		AdQSM	AdTree	TreeQSM	AdQSM	AdTree	TreeQSM
Absolute error	Small-Leafed Olive_Avg(m)	0.0192	0.1045	**0.0094**	0.0352	0.1312	**0.0337**
	Small-Leafed Olive_noise_Avg(m)	0.0193	0.1067	**0.0139**	0.0467	0.132	**0.0419**
	Flamboyant Tree_Avg(m)	0.262	**0.2433**	0.3421	**0.199**	0.2496	0.54
	Flamboyant Tree_Avg_noise(m)	0.2876	**0.2411**	0.3491	**0.1703**	0.2482	0.6145
	Fir Tree_Avg(m)	**0.0539**	0.0573	0.0543	0.0878	0.1213	**0.0597**
	Fir Tree_Avg_noise(m)	**0.0524**	0.0765	0.0855	0.5154	0.1762	**0.0819**
	Ajiang Olive_Avg(m)	0.1592	0.1264	**0.107**	**0.1074**	0.3869	0.1706
	Ajiang Olive_Avg_noise(m)	0.2167	0.1896	**0.1614**	**0.1435**	0.5692	0.2232
	Camphor Tree_Avg(m)	0.1314	0.1421	**0.0725**	0.18	0.2693	**0.0984**
	Camphor Tree_Avg_noise(m)	0.0955	0.1288	**0.0643**	0.1695	0.3025	**0.0791**
	tree Avg(m)	0.1297	0.1416	**0.126**	**0.1655**	0.2586	0.1943
Relative error	Small-Leafed Olive_Avg	0.0019	0.0103	**0.0009**	0.0035	0.0129	**0.0033**
	Small-Leafed Olive_noise_Avg	0.0019	0.0105	**0.0014**	0.0046	0.013	**0.0041**
	Flamboyant Tree_Avg	0.0018	**0.0017**	0.0024	**0.0014**	0.0017	0.0037
	Flamboyant Tree_Avg_noise	0.002	**0.0017**	0.0024	**0.0012**	0.0017	0.0043
	Fir Tree_Avg	**0.0029**	0.0031	**0.0029**	0.0048	0.0066	**0.0032**
	Fir Tree_Avg_noise	**0.0028**	0.0042	0.0046	0.028	0.0096	**0.0044**
	Ajiang Olive_Avg	0.0035	0.0028	**0.0024**	**0.0024**	0.0086	0.0038
	Ajiang Olive_Avg_noise	0.0048	0.0042	**0.0036**	**0.0032**	0.0126	0.0049
	Camphor Tree_Avg	0.0032	0.0034	**0.0018**	0.0044	0.0065	**0.0024**
	Camphor Tree_Avg_noise	0.0023	0.0031	**0.0016**	0.0041	0.0073	**0.0019**
	tree Avg	0.0027	0.0045	**0.0024**	0.0057	0.0081	**0.0036**

vegetation reconstruction. Extensive validations were conducted using 10 selected tree species from the dataset, employing both noisy and noise-free data, to assess the computational accuracy of Three state-of-the-art algorithms: AdTree, AdQSM, and TreeQSM. These tests covered tree reconstruction, skeleton point extraction, and quantitative structure calculation, affirming the dataset's efficacy in algorithmic evaluations.

Acknowledgements

This work was supported in part by the National Key Research and Development Program of China (Project No. 2022YFB3903700), Research Project of Shenzhen S and T Innovation Committee (Project Nos. JCYJ20210324093012033, KJZD20230923115508017), Natural Science Foundation of Guangdong Province (Project No. 2024A1515030061) and Research project of State Key Laboratory of Subtropical Building and Urban Science(Project No. 2023ZB18).

References

Du, S., Lindenbergh, R., Ledoux, H., Stoter, J., Nan, L., 2019. AdTree: accurate, detailed, and automatic modelling of laser-scanned trees. *Remote Sensing*, 11(18), 2074.

Fan, G., Nan, L., Dong, Y., Su, X., Chen, F., 2020. AdQSM: A new method for estimating above-ground biomass from TLS point clouds. *Remote Sensing*, 12(18), 3089.

Ferrara, R., Virdis, S. G., Ventura, A., Ghisu, T., Duce, P., Pellizzaro, G., 2018. An automated approach for wood-leaf separation from terrestrial LIDAR point clouds using the density based clustering algorithm DBSCAN. *Agricultural and forest meteorology*, 262, 434–444.

Hu, S., Li, Z., Zhang, Z., He, D., Wimmer, M., 2017. Efficient tree modeling from airborne LiDAR point clouds. *Computers & Graphics*, 67, 1–13.

Kankare, V., Holopainen, M., Vastaranta, M., Puttonen, E., Yu, X., Hyyppä, J., Vaaja, M., Hyyppä, H., Alho, P., 2013. Individual tree biomass estimation using terrestrial laser scanning. *ISPRS Journal of Photogrammetry and Remote Sensing*, 75, 64–75.

Liu, Y., Guo, J., Benes, B., Deussen, O., Zhang, X., Huang, H., 2021. TreePartNet: neural decomposition of point clouds for 3D tree reconstruction. *ACM Transactions on Graphics*, 40(6).

Mei, J., Zhang, L., Wu, S., Wang, Z., Zhang, L., 2017. 3D tree modeling from incomplete point clouds via optimization and L 1-MST. *International Journal of Geographical Information Science*, 31(5), 999–1021.

Putman, E. B., Popescu, S. C., 2018. Automated estimation of standing dead tree volume using voxelized terrestrial lidar data. *IEEE Transactions on Geoscience and Remote Sensing*, 56(11), 6484–6503.

Raumonen, P., Kaasalainen, M., Åkerblom, M., Kaasalainen, S., Kaartinen, H., Vastaranta, M., Holopainen, M., Disney, M., Lewis, P., 2013. Fast automatic precision tree models from terrestrial laser scanner data. *Remote Sensing*, 5(2), 491–520.

Vega, C., Hamrouni, A., El Mokhtari, S., Morel, J., Bock, J., Renaud, J.-P., Bouvier, M., Durrieu, S., 2014. PTrees: A point-based approach to forest tree extraction from lidar data. *International Journal of Applied Earth Observation and Geoinformation*, 33, 98–108.